
A NUMERICAL STUDY ON THE CONTROL OF THE FLOW IN AN AXISYMMETRIC SUDDEN EXPANSION

Kürşad Melih GÜLEREN*

Flight Training Department, Faculty of Aeronautics and Astronautics, Anadolu University, Eskişehir, Turkey

ABSTRACT

A numerical study on the control of the flow and its characteristics in an axisymmetric sudden expansion have been performed considering some stability parameters; including velocity profile modification, wall-shaping and blowing/suction. Due to the fact that numerous cases were tested, the flow was assumed to be two-dimensional, incompressible and laminar in order to use computational time feasibly. The implemented numerical method was validated with the previous experimental and numerical data. Flow characteristics regarding the pitchfork-bifurcation, velocity variations, separation and stain rate relationship, pressure and skin friction coefficients are examined in detail. It was seen that all stability parameters have favourable or adverse effect on the flow asymmetry. The blowing modification has been found to turn the asymmetric flow into symmetric flow provided that adequate blowing mass flow is applied.

Keywords: Flow control, Axisymmetric flow, Sudden expansion, Computational fluid dynamics

1. INTRODUCTION

Sudden expansion flow problems are commonly encountered in many engineering applications such as orifices, diffusers, heat exchangers, burners, combustion chambers, cooling systems for turbine blades and electronics, building designs with wind loading and many flow-relevant systems. The flow behaviour regarding separation and reattachment is quite complex phenomena and covers the entire flow physics in the downstream of the sudden expansion. Incompressible laminar flows in two-dimensional sudden expansions preserves a perfectly symmetric shape with two identical separation region on two sides of the sudden expansion up to a critical Reynolds number. At higher Reynolds numbers, the asymmetry of the steady flow arises due to a symmetry-breaking bifurcation. This bifurcation entails the fact that one of the separation bubbles is larger than the other one which can take place on either side of the channel without any preference. Further increasing the Reynolds number causes a third separation bubble to emerge at downstream of the smaller bubble and many more depending on the expansion ratio.

1.1. Studies Regarding the Flow Physics

The intriguing aspect of the sudden expansion flows and their importance in engineering applications have attracted the interest of many scientists and researchers for a long time. In the last fifty years or so, a substantial amount of experimental and numerical research has been published. Experimental investigations of these flows [1-6] suggested that the asymmetry observed in axisymmetric sudden expansion was caused by disturbances generated at the corners of the expansion and increased in the shear layers. In the study of [6], another explanation for the asymmetry by stating was proposed that the flow undergoes a symmetry-breaking pitchfork bifurcation causing the symmetric solution unstable. They noted that the larger recirculation zone could take place on either side of the wall which means that there are two numerical solutions providing same information for the flow characteristics of the pitchfork bifurcation.

*Corresponding Author: kmguleren@anadolu.edu.tr

Pioneering numerical studies of sudden expansion flows [7-9] focused on the symmetry-breaking bifurcation which was experimentally studied later by [6] and numerically investigated by [10]. The effect of the expansion ratio on the symmetry-breaking bifurcation was numerically studied by [11-13]. Commonly, these studies confirmed the separation bubbles and the flow asymmetry which were observed experimentally. These numerical studies noted also that flow stability was improved when the expansion ratio was reduced and the three-dimensional effects were increased when the aspect ratio was decreased.

1.2. Studies Regarding the Control of the Flow

In spite of the ample studies for axisymmetric sudden expansion flows discussing various parameters of the flow physics, little effort has been given to the control of these flows. Mostly, passive and active control attempts regarding the flow separation are limited to the flow behind a backward-facing step (BFS). For example; a normal mass bleeding from the lower wall of BFS was studied and found out that reverse flow rate decreased with normal injection [14]. More recently, similar studies were performed including the effect of suction [15-16]. The reattachment length was increased by increasing blowing bleed rate and was decreased by increasing suction bleed rate [15]. Both blowing and suction were able to reduce the length of the separation zone [16]. This dissimilarity is due the fact that the Reynolds number in the work of [15] was much less than that of [16].

One of the active control methods of the flow in axisymmetric sudden expansion is converting the sudden expansion geometry into a gradually expanded geometry or i.e. diffuser. A common purpose of this control method is to reduce the separation and thus regain pressure. Among many, probably the most noteworthy study was performed by [17]. They reported velocity measurements in diffusers with angles varying from 10° to 90° and observed that a decrease in diffuser angle shortens the recirculation flow region and reduces the magnitude of the streamwise velocity inside that region.

Modification of inflow also has a considerable effect on the control of the flow in sudden expansion. The effect of parabolic and uniform inlet velocity profile on the onset of the bifurcation was investigated [18]. It was found that uniform inflow had a tendency to stabilize the asymmetric solution by delaying the onset of bifurcation to higher Reynolds number, but it was not possible to eliminate the flow asymmetry totally. [19], on the other hand, could manage to establish the flow symmetry by imposing a sinusoidal variation of inlet velocity profile.

1.3. Present Study

The aim of the present work is to examine the effect of some control parameters such as inflow modification, shaping and blowing/suction in an axisymmetric sudden expansion. In spite of some numerous works performed for the control of the flow subjected to backward-facing step, the open literature has not yet elaborately explored for the flow control in symmetric sudden expansion. However; it should be noted that the present work does not include all the aspects of the control mechanisms, it focuses rather some of the particular cases which have not been studied yet. For instance, the inflow with respect to different inlet boundary layers has not discussed before. In terms of shaping, asymmetric shaping is discussed along with the gradually inclined walls. Blowing and suction is also applied differently from the way that usually exists in the literature; instead of using upper or lower walls, the lateral walls just above and under the inlet are used for blowing and suction injections.

2. METHODS AND MATERIALS

The geometric model for the axisymmetric sudden expansion is shown in Figure 1a. The expansion ratio for the model is 3:1 (D/d). Upstream (l/d) and downstream lengths (L/d) of the sudden expansion are considered as 5 and 75, respectively. The Reynolds number is defined as $Re_c=U_c d/\nu$ where U_c is the centreline velocity at the start of the sudden expansion ($x/d=0$) and ν is the kinematic viscosity. The adopted computational mesh for the expansion model is a structured mesh and has 124 000 rectangular cells. A closed view of the computational mesh around inlet is demonstrated in Figure 1b. In this study, the ratio of the distances between the consecutive cells is defined as the spacing ratio (SR). For the upstream region of the sudden expansion, 40 cells are placed along the y-axis ($-0.5 \leq y/d \leq 0.5$) with $SR=1.1$. The nearest cell to the wall is 0.00435 d long and the distance between the cells located at the centre is 0.05 d. Along the x-axis for the upstream region ($-5 \leq x/d \leq 0$), 100 cells are placed with $SR=1.025$. Downstream of the sudden expansion, 300 cells with $SR=1.01$ are spread along the x-direction till $x/d=25$. Another 200 cells, which are uniformly spaced, are set for the rest of the domain. Along the y-direction, the cells at $-0.5 \leq y/d \leq 0.5$ follow as the same structure as those for upstream region. On the other hand, the cells at $-1.5 \leq y/d \leq -0.5$ and $0.5 \leq y/d \leq 1.5$ are uniformly spaced.

At the inlet, the Blasius Solution [20] is implemented to describe the velocity profile. The boundary layer thickness δ is defined as the closest distance between the wall and the location where the axial velocity U is equal to the centre velocity U_c . For instance, $\delta/d=0.5$ indicates that the boundary layer thickness is equal to half of the upstream channel width d which implies a laminar fully developed velocity profile. Six boundary layer cases ($\delta/d=0.02$, $\delta/d=0.1$, $\delta/d=0.2$, $\delta/d=0.3$, $\delta/d=0.4$, and $\delta/d=0.5$) are analysed for thirteen different Reynolds numbers of 75, 82.5, 90, 100, 112.5, 135, 150, 165, 187.5, 225, 262.5, 337.5 and 380. These cases are repeated for the control parameters presented in this paper. Because it is not feasible to show all the results of these numerous cases, only the significant ones are shown and discussed. Regarding the boundary conditions, zero-velocity is employed at the walls. At the exit, zero-diffusion flux is applied for all flow variables with the correction of overall mass balance. This boundary condition requires the fully developed stage of the flow which is achieved for our cases well before $x/d=75$ where the outlet boundary condition is set.

The tensor forms of steady-incompressible continuity (1), momentum (2) and energy equations (3) solved in this present work read as:

$$\frac{\partial u_i}{\partial x_i} = 0 \quad (1)$$

$$\rho u_j \frac{\partial u_i}{\partial x_j} = -\frac{\partial p}{\partial x_i} + \mu \frac{\partial^2 u_i}{\partial x_j^2} \quad (2)$$

$$\frac{\partial}{\partial x_i} (\rho u_i h) = \frac{\partial}{\partial x_j} \left(\frac{k}{C_p} \frac{\partial h}{\partial x_j} \right) \quad (3)$$

The enthalpy is calculated as $h = \int_{T_{ref}}^T C_p dT$. Density ρ , dynamic viscosity μ , specific heat C_p and thermal conductivity k vary with respect to temperature for the working fluids as will be shown later in this study.

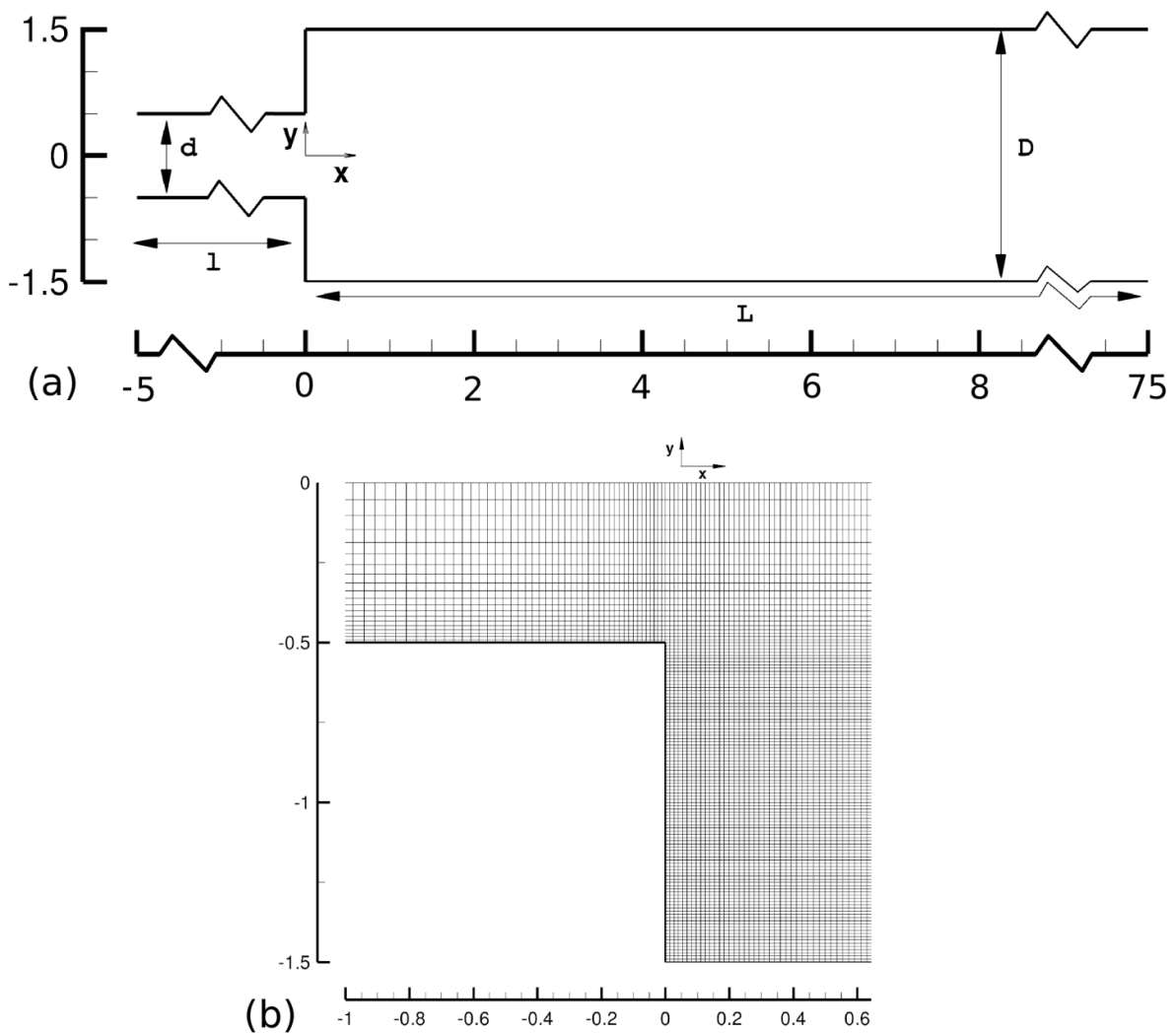


Figure 1. The geometric model of axisymmetric sudden expansion (a) and a closed view of the mesh around inlet (b)

These governing differential equations are solved via a finite volume code [21], which is based on the projection method [22]. The convective terms in (2) and (3) are discretized using QUICK scheme [23], pressure-velocity coupling is accomplished using the SIMPLEC algorithm [24] and PREssure Stagging Option (PRESTO) scheme [25] is used for the pressure interpolation. The set of linearized equations are solved by the Gauss–Seidel method, which is coupled with an algebraic multigrid method to accelerate convergence. All computations are converged to residuals less than 10^{-5} .

3. RESULTS

3.1. Validation

The adopted code and thus the numerical method in this study are validated with the experimental data [3] and also with the numerical predictions [13, 26]. In Figure 2a, predicted axial velocity profiles are compared with the experimental counterparts of [3] for $Re_c=380$ at axial locations of $x/d=-0.25, 1.5, 2.5, 5, 10, 12.5, 15$ and 20 . Current predictions agree well with the experimental data except for the stations of $x/d=15$ and 20 where some minor discrepancies are observed. These discrepancies are attributed to the three-dimensional effects caused by the experimental set-up (Figure 14., p.120, [3]). They also observed some fluctuations in the flow causing around 1-2 % turbulent intensity. This level of turbulence

could be also responsible for these discrepancies. One should keep in mind that the Reynolds numbers studied in this work are lower than $Re_c=380$. Therefore, it would be fair to say less discrepancies are expected for lower Reynolds numbers.

The detachment and reattachment locations of the separation bubbles are displayed as a function of Reynolds number in Figure 2b. Current predictions agree well with the predictions of [13, 26]. The critical Reynolds number Re_{cr} , which represents the onset of the pitchfork bifurcation, is found as 85. For $Re_c < 85$, separation bubbles have the same length ($x_1=x_2$). Whereas for $Re_c > 85$, the reattachment length of smaller bubble x_2 decreases slightly till $Re_c = 120$ and then becomes almost independent of Re_c . The reattachment length of larger bubble x_1 increases monotonically with Re_c . For $Re_c > 150$, a third separation bubble is formed as illustrated at the top of Figure 2b. Detachment and reattachment locations for this bubble are represented by x_3 and x_4 , respectively. The difference between x_4 and x_3 indicates the length of this separation bubble which increases as Reynolds number increases.

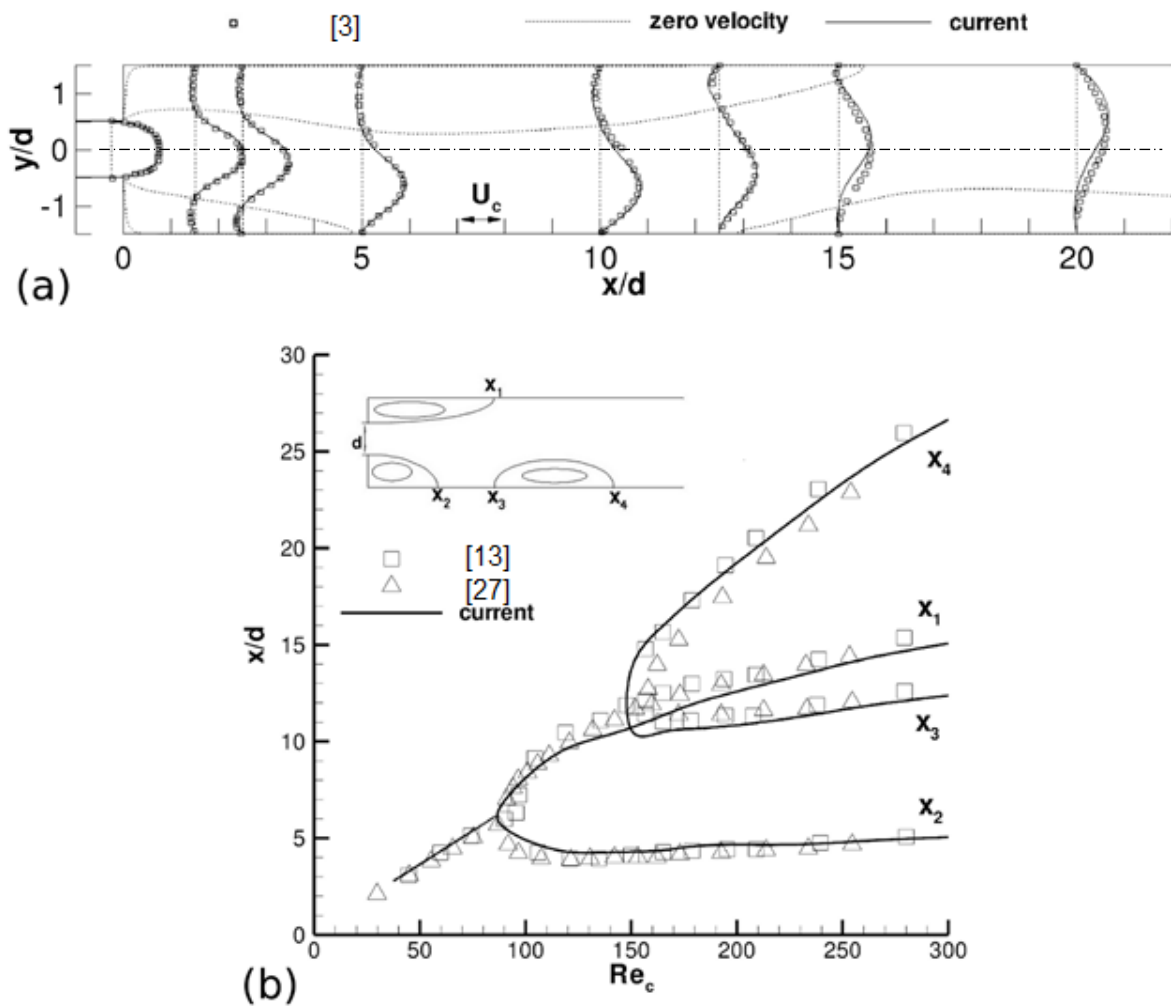


Figure 2. Axial velocity profiles U/U_c at $Re_c=380$ (a) and bifurcation characteristics (b)

3.2. The Effect of Initial Function

Determination of bifurcation characteristics numerically, in fact, is not a straightforward task. One needs to be very careful or frankly sceptical about the adopted solver as well as the initial function (guess function) used to solve the sudden expansion flow problem correctly. According to [18], an implicit solver of stream-function vorticity formulation can recover the unstable symmetric solution or the stable

asymmetric solution depending on whether the initial guess is symmetric or not. In the present case, adopted flow solver recovers mostly the stable asymmetric solution except for a special circumstance where the flow is on the verge of producing another separation bubble in addition to the asymmetric two. Choosing an inappropriate initial function might cause a symmetric unstable solution. This, in turn, culminate in a wrong calculation of Re_{cr} and hence a misinterpretation of bifurcation characteristics. In order to assess the effect of initial function for the axial velocity, ten different initial functions are tested for the case $\delta/d=0.02$ at $Re_c=380$. The functions are chosen considering the fact that they have axis¹ or origin symmetry². The functions and their performance are tabulated in Table 1. None of the functions related with the x-coordinate namely F1, F2 and F5 converges to the asymmetric solution. As for the y-coordinate; asymmetric functions (F4 and F8) converge to the asymmetric solution which is managed only by the signum function (F7) among symmetric functions (F3, F6 and F7). Considering the number of iteration for convergence, the asymmetric y-function in conjunction with cubic polynomial should be preferred as the first choice for the initial function provided that the function obtained from the converged solution of the case $\delta/d=0.5$ (F10) is not available yet. A random field between 0 and 1 converges faster than F8 and F10 but ends up with a symmetric unstable solution. Briefly, the initial function should be a function of y-coordinate without axis or origin symmetry to guarantee the asymmetric stable solution.

Table 1. The effect of initial function to the solution for the case $\delta/d=0.02$ at $Re_c=380$

Function	Required Iteration for Convergence	Converged to Asymmetric Solution	Symmetry
F1 (X/L) ²	2048	NO	Y-axis
F2 (X/L) ² -(X/L)-1	4269	NO	NO
F3 (Y/D) ²	4860	NO	X-axis
F4 (Y/D) ² -(Y/D)-1	6296	YES	NO
F5 1/(X/L)	7023	NO	Origin
F6 1/(Y/D)	8146	NO	Origin
F7 sgn(Y)	5883	YES	Origin
F8 (Y/D) ³	4916	YES	NO
F9 Rand(0,1)	2015	NO	NO
F10 From the converged velocity field of the case $\delta/d=0.5$	4818	YES	NO

¹ $f(a) = f(-a)$

² $f(-a) = -f(a)$

3.3. Inflow Modification

The effects of inlet boundary layer on axial velocity profiles are displayed for three Reynolds numbers in Figure 3. Each Reynolds number indicates different bifurcation characteristics as pointed out in Figure 2b. For the investigated Reynolds number; velocity profiles of the case $\delta/d=0.5$ are quite close to those of the case $\delta/d=0.2$, but they differ substantially from those of the case $\delta/d=0.02$. At $Re_c=75$, maximum velocity located at the centre decreases by 16 % (from $0.86 U/U_c$ at $\delta/d=0.5$ to $0.72 U/U_c$ at $\delta/d=0.2$). This difference gets more pronounced at $x/d=10$, where it decreases by 36 % from 0.55 to $0.35 U/U_c$. At $Re_c=135$, it is noticeable that the predictions at $x/d=5$ overlap each other near the bottom wall where no back-flow exist. Away from the wall, discrepancies increase gradually to a peak value and then decrease near the other wall. This scenario is reversed when the flow change direction at $x/d=12.5$. At $Re_c=225$, the flow is directed towards the bottom wall first and then the top wall afterwards. Similar to the cases for $Re_c=75$ and $Re_c=135$, minor differences are observed in velocities between the cases $\delta/d=0.5$ and $\delta/d=0.2$ and major ones between the cases $\delta/d=0.5$ and $\delta/d=0.02$.

It should be noted that as the boundary layer changes, total mass flow rate of the channel is changed. As compared $\delta/d=0.5$, the mass flow rate increases by 10, 20, 30, 40 and 48 per cent for $\delta/d=0.4$, $\delta/d=0.3$, $\delta/d=0.2$, $\delta/d=0.1$ and $\delta/d=0.02$, respectively.

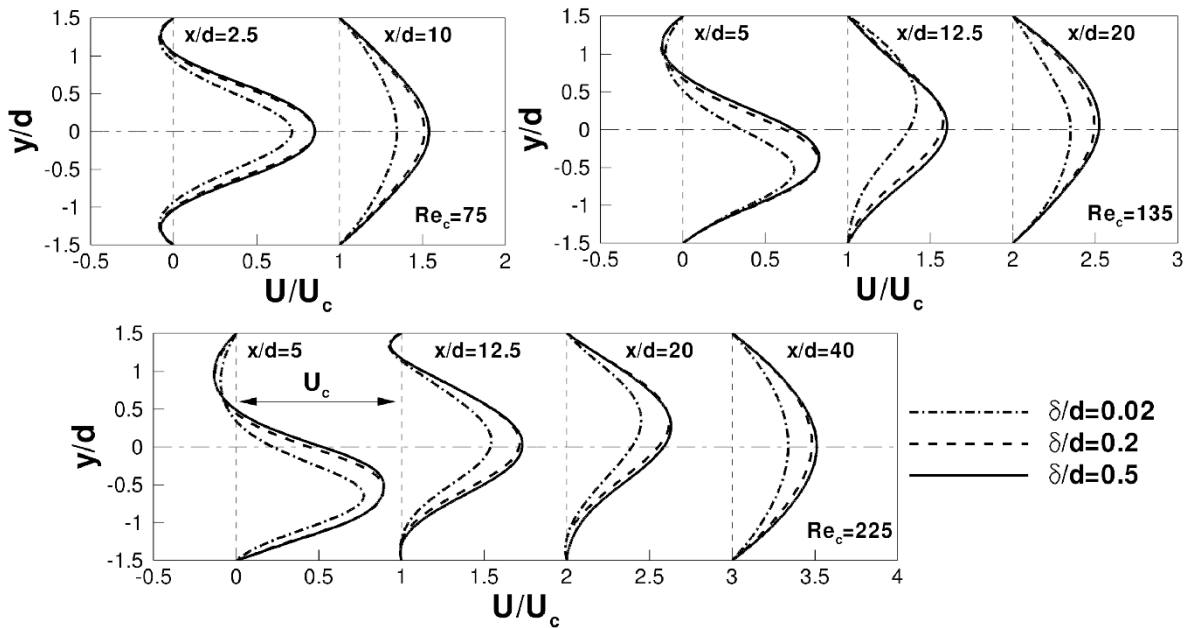


Figure 3. The effects of inlet boundary layer on axial velocity profiles for different Reynolds numbers

In this study, the asymmetry of the flow is presented by the ordinate of the maximum velocity ($y@U_{max}$) in the computational domain. In Figure 4a, the ordinate of U_{max} is shown for the case $\delta/d=0.5$. At $Re_c=25$, since the flow is perfectly symmetric, the ordinate is zero. At $Re_c=90$ the flow is observed to be highly asymmetric. First the flow impinges the bottom wall and later the upper wall. After these two hits, the flow loses most of its momentum and consequently oscillates near the centre when $x/d>20$. Figure 4a also exhibits that as Re_c increases the maximum and minimum peaks of the ordinate increase in absolute sense which causes significant augmentation of the flow instability. For example, the first peak is located at $y=-0.55$ for $Re_c=90$, at $y=-0.75$ for $Re_c=225$, and $y=-0.83$ for $Re_c=337.5$. In a similar manner, the second peak is placed at $y=0.36$ for $Re_c=90$, at $y=0.54$ for $Re_c=225$, and $y=0.68$ for $Re_c=337.5$. In order

to determine the degree of the asymmetry in the sudden expansion flows, the author proposes a simple formula called as “The Magnitude of Asymmetry (MA)”. This parameter is formulated in such a way that the value '0' indicates a perfect symmetry and '1' stands for the maximum asymmetry of the flow. MA is defined as the ratio of the sum of the absolute values of the peak ordinates (maximum and minimum) to the expansion ratio (ER). Taking into account only two dimensional effects, MA can be written as:

$$MA = \frac{(|y_{max}| + |y_{min}|)/d}{ER} \quad (4)$$

In the case $\delta/d=0.5$, MA is calculated as 0 for $Re_c=25$, 0.3 for $Re_c=90$, 0.43 for $Re_c=225$, and 0.5 for $Re_c=337.5$. Since, the maximum Reynolds number investigated here is limited to $Re_c=337.5$, maximum MA is found as 0.5. One might ask whether it is possible to exceed 0.5 or MA formulation should be modified for the cases of finite aspect ratio. However, these are out of the scope of the current study and will be handled in the near future by considering three dimensional and turbulence effects. Figure 4b indicates that inlet boundary layers have moderate effects on the asymmetry. For example, MA for the case $\delta/d=0.5$ was calculated as 0.5 at $Re_c=337.5$. MA decreases to 0.47 (6 % change) for the case $\delta/d=0.2$ and to 0.42 (16 % change) for the case $\delta/d=0.02$ at the same Reynolds number.

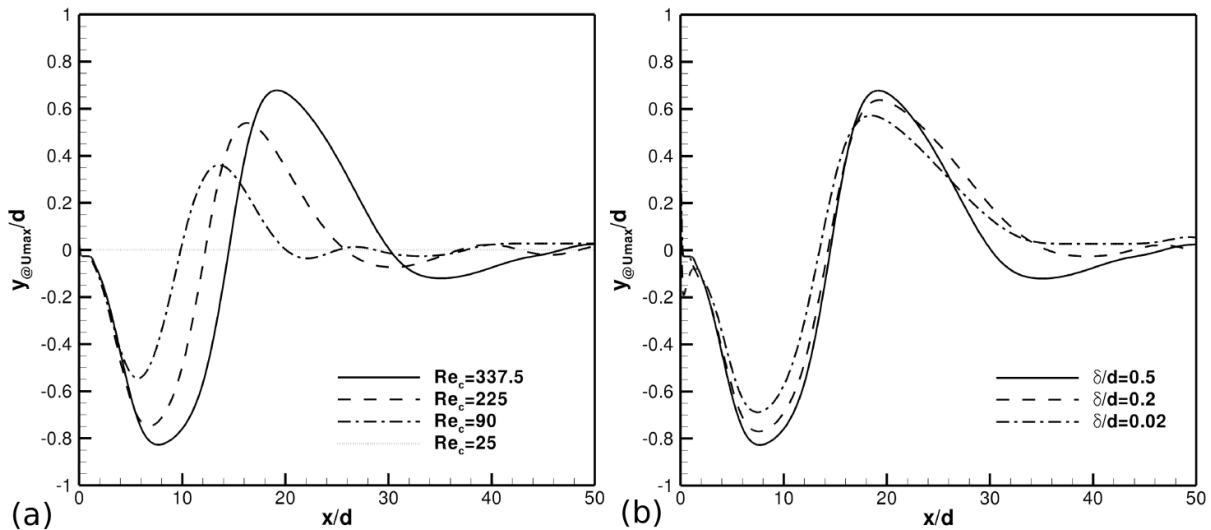


Figure 4. Variation of the location of maximum axial velocity $y@U_{max}/d$. The effects of Reynolds number at $\delta/d=0.5$ (a) and the inlet boundary layer at $Re_c=337.5$ (b)

The variation of pressure coefficient (C_p) on the upper and lower walls is presented in Figure 5. The variation of C_p on the walls can be analysed in 5 different regions. On both walls, there is almost no change of C_p in Region I where the flow is separated. Close to the reattachment, C_p increases rapidly due to a sharp adverse pressure gradient (Region II). Following this rapid increase, C_p values on both walls reach peak values at $x/d \approx 8$ for the bottom wall and at $x/d \approx 20$ for the top wall. After the recovery from separation, the flow accelerates quickly corresponding to sudden decrease of C_p (Region III). As for Region IV, there is a moderate increase of C_p . This increase can be explained by examining back the Figure 4b. It can be inferred from this figure that, the main flow is directed upward at $x/d \approx 8$ which entails the main flow to lose its energy and hence to decelerate near the bottom wall. Likewise, the main flow is directed in this case downward at $x/d \approx 20$ causing a deceleration near the top wall. In Region V, the flow recovers from all separation zones and starts to progress a stability character. C_p values on the top and bottom walls overlap each other (also see Figure 10., p.326 in [26]) and decrease monotonically

corresponding to the fully developed stage of the flow. Decreasing the thickness of the inlet boundary layer causes a significant rise of (C_p) from inlet to outlet of the sudden expansion with an exception of Region I on the bottom wall. As the flow progress and reaches the fully developed stage, this rise can be observed more easily. For example at the outlet, C_p is calculated as 0.15 for the case $\delta/d=0.5$. It increases by 60 % for the case $\delta/d=0.2$ and by 85 % for the case $\delta/d=0.02$.

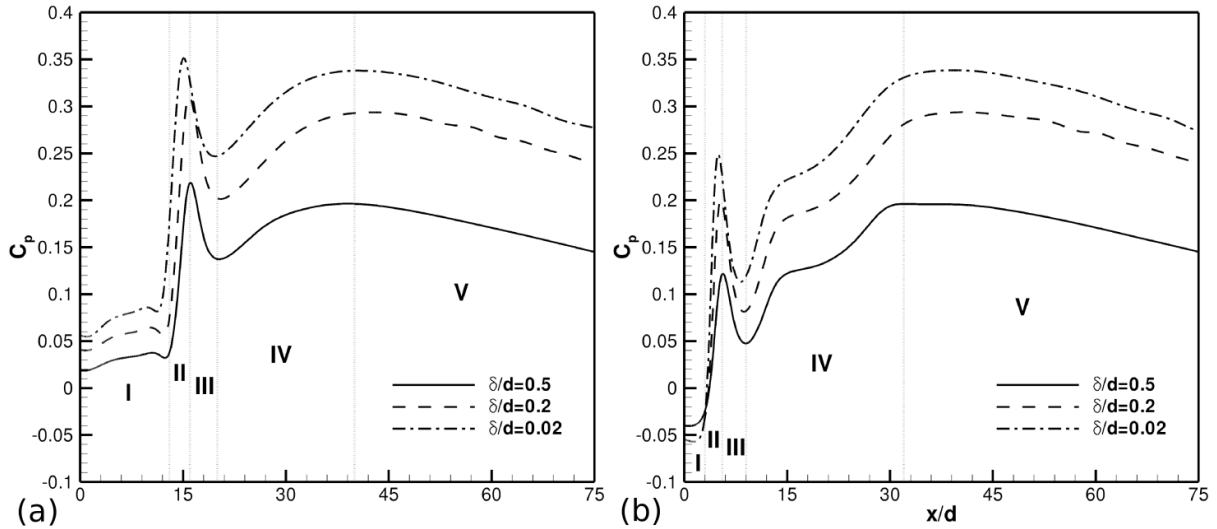


Figure 5. Variation of pressure (C_p) on the top wall (a) and the bottom wall (b) at $Re_c=337.5$

3.4. Shaping

As is well known, one of the active control methods is to guide the flow by modifying the shape of the geometry for which the flow is subjected to. In this case, a shaping angle is introduced as shown in Figure 6. For the original case of sudden expansion, the shaping angle α_s equals to zero. At $Re_c=380$, axial velocity contours are presented in Figure 6a for the original case. For $\alpha_s=85^\circ$, the separation zones placed near the lower wall almost disappear, whereas the separation zone near the top wall is still visible but delayed approximately $5d$ downstream as seen in Figure 6b. Here the size of separation zone is estimated to decrease by 63 % compared to the original sudden expansion case. Adjusting the shaping angle at 75° reduces the size of these back-flow regions only by 39 %. Along with linear shaping employed for these two cases, a second order parabolic shaping is also utilized to see whether convex wall adaptation makes any improvement in controlling the separation. However, separation zones still exist as seen in Figure 6d and are reduced by 26 % which is less than the linear shaping. Therefore, parabolic shaping does not improve the flow stability but it delays the detachment around 2-3d downstream. Lastly, only one side of the sudden expansion is shaped and the other is kept untouched. As seen in Figure 6e, the back-flow regions are very similar to the original case but still these zones are reduced by 12 %.

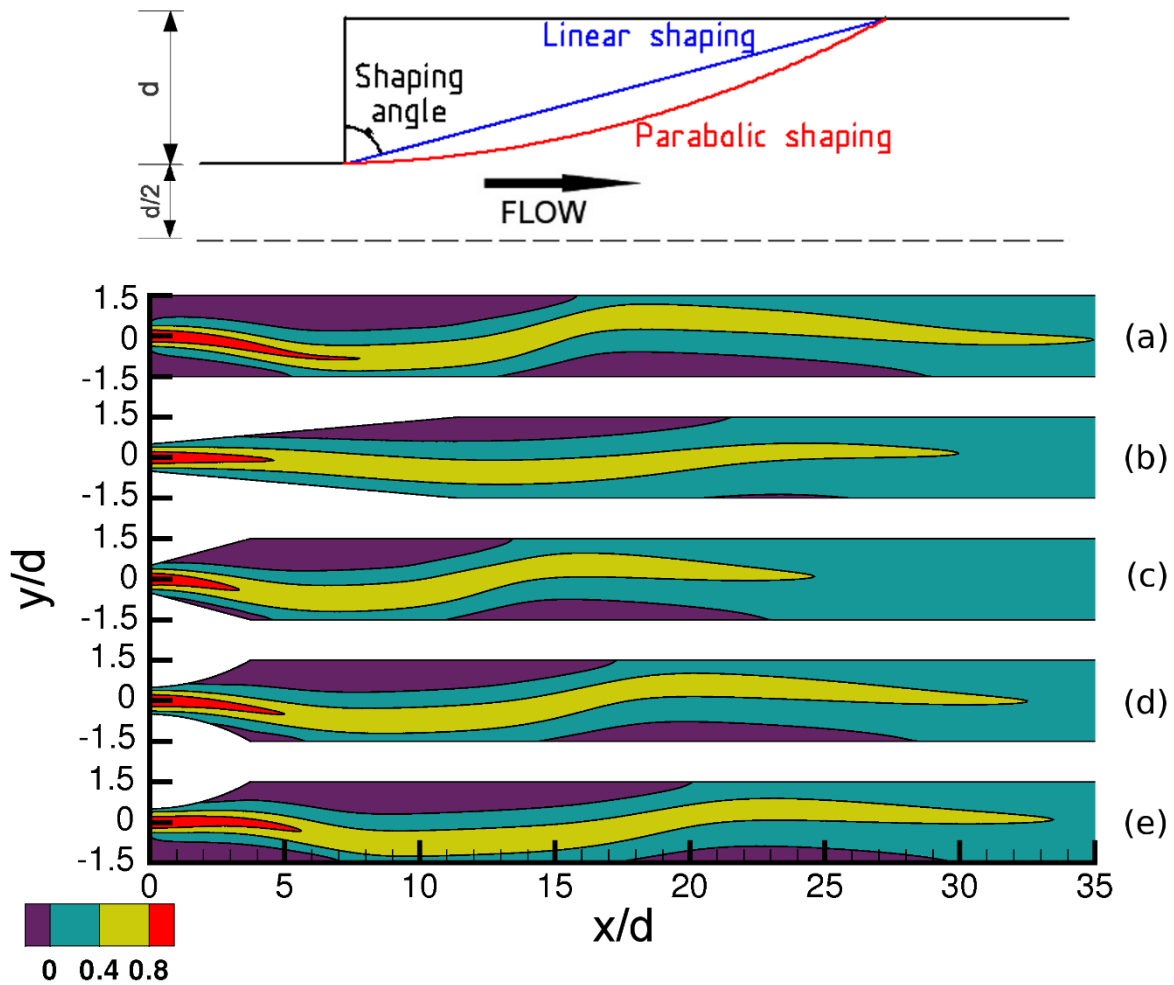


Figure 6. Axial velocity contours at $Re_c=380$ for various sudden expansion configurations. Original shape (a), linear shaping with $\alpha_s=85^\circ$ (b), linear shaping with $\alpha_s=75^\circ$ (c), parabolic shaping of the previous case (d), asymmetric parabolic shaping (e).

3.5. Blowing / Suction

Another active method namely blowing/suction is applied on the surfaces above and below the inlet as represented by arrows (totally six arrows) which are equally spaced. Four different blowing and suction conditions are applied at $Re_c=380$ where the Reynolds number of the channel becomes $Re=252$. For suction, the ratio of the mass flow rate at suction to that at the inlet (m_s/m_i) is assumed as 0.18, 0.27, 0.36 and 0.54. For these cases, axial velocity contours are shown in Figure 7. Likewise, axial velocity contours of different blowing cases (m_b/m_i) of 0.18, 0.27, 0.315 and 0.36 are shown in Figures 9. The width of the blowing and suction is 5 per cent of the upstream channel height d and the velocity profiles are parabolic similar to the channel inlet. In the case of blowing and suction, total mass flow rate of the channel is changed and so the Reynolds number. Re equals to 207, 184, 161 and 116 for the suction ($m_s/m_i=0.18, 0.27, 0.36$ and 0.54); 297, 320, 331 and 343 for the blowing cases ($m_b/m_i= 0.18, 0.27, 0.315$ and 0.36).

As seen in Figure 7, as the suction starts another back-flow region emerges on the upper wall between $x/d=26$ and $x/d=32$. This region enlarges and moving upstream as the suction flow rate increases. The jet and the back-flow regions recede back to the inlet as the suction rate gets stronger. For $m_s/m_i=0.18$,

total size of back-flow regions increases by 11 % in comparison to the original case. This value increases very slowly so that it becomes 14 % at $m_s/m_i=0.54$. In spite of the fact that the jet gets weaker and the back-flows moves close the inlet, the flow becomes more asymmetric due to the presence of the fourth separation zone.

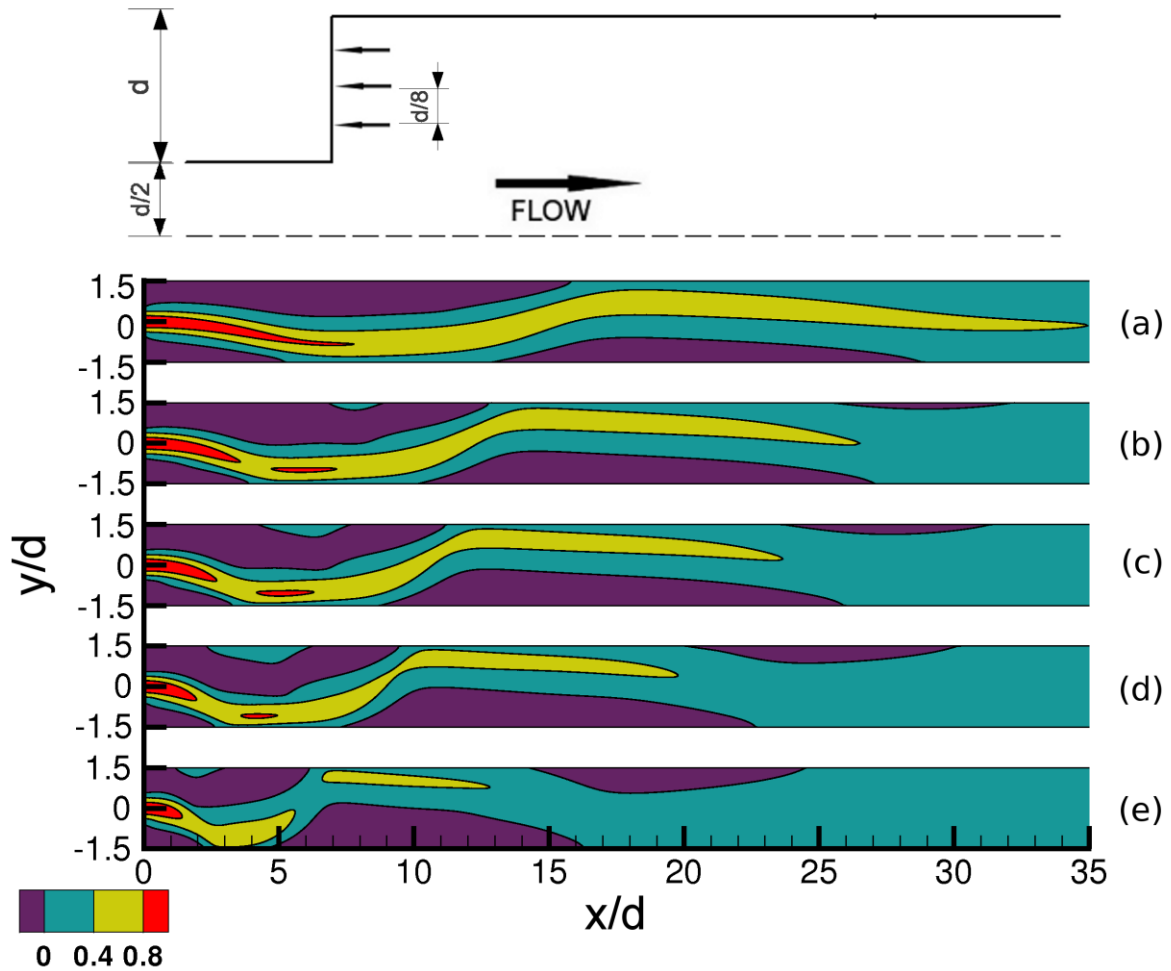


Figure 7. Axial velocity contours at $Re_c=380$ for various suction configurations. Reference case of $m_s/m_i = 0$ (a), case of $m_s/m_i = 0.18$ (b), case of $m_s/m_i = 0.27$ (c), case of $m_s/m_i = 0.36$ (d), case of $m_s/m_i = 0.54$ (e).

In order to assess the asymmetry of the quantitatively, the ordinate of U_{max} is presented in Figure 8 for the cases shown in the previous picture. It is noticeable that as the suction rate increases the peak ordinates increase suggesting that the flow becomes more unstable by approaching the walls much more. It is actually so strong that the ordinate of the third peak increases almost 5 fold by increasing the rate from $m_s/m_i=0.18$ to $m_s/m_i=0.54$. As shown also by arrows, the axial locations of U_{max} reduce indicating that the separation bubbles move upstream as the suction rate increases. This, however, does not provide any improvement in flow stabilization since the ordinates in Figure 8 dampen to zero almost at the same axial locations for all cases.

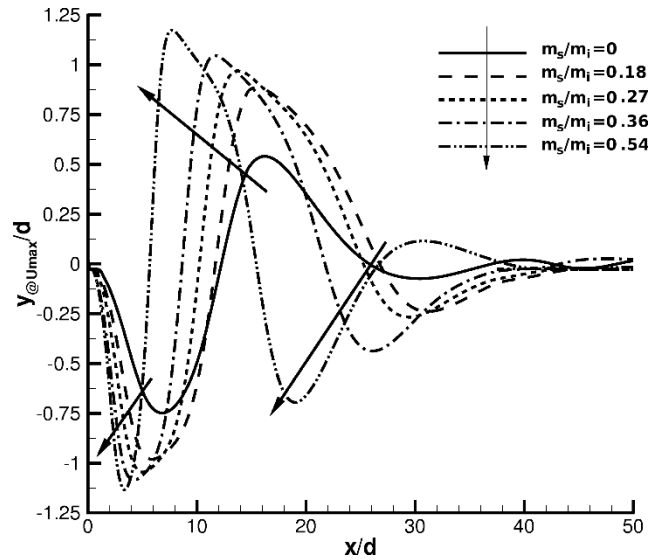


Figure 8. Variation of the location of maximum axial velocity $y@U_{max}/d$ for the suction cases

In Figure 9, the effect of the blowing rate is shown. With the start of the blowing, the back-flow regions are swept along the main flow direction with decreasing in size. At $m_b/m_i=0.18$, the size of the back-flow is decreased by 40 %. Thereafter, it is decreased by 72 % and % 95 for $m_b/m_i=0.27$ and $m_b/m_i=0.315$, respectively. At $m_b/m_i=0.36$, back-flow regions almost disappear as shown in Figure 8e except the inlet region for which a zoomed view is shown on the right top of the main figure. Two small counter rotating vortex pairs are located just above and below the middle blowing jet. These vortex pairs are in conjunction with small-back flow regions which exist between blowing jets. Two more but larger vortices are also observed; one is located near the wall and the other is placed between the main jet and the blowing jet which is the closest one to centre of sudden expansion. The underlying cause as to why these vortices are much larger is because the blowing jets except the middle one are drifted toward to the middle jet as a result of the so-called “Coanda effect”.

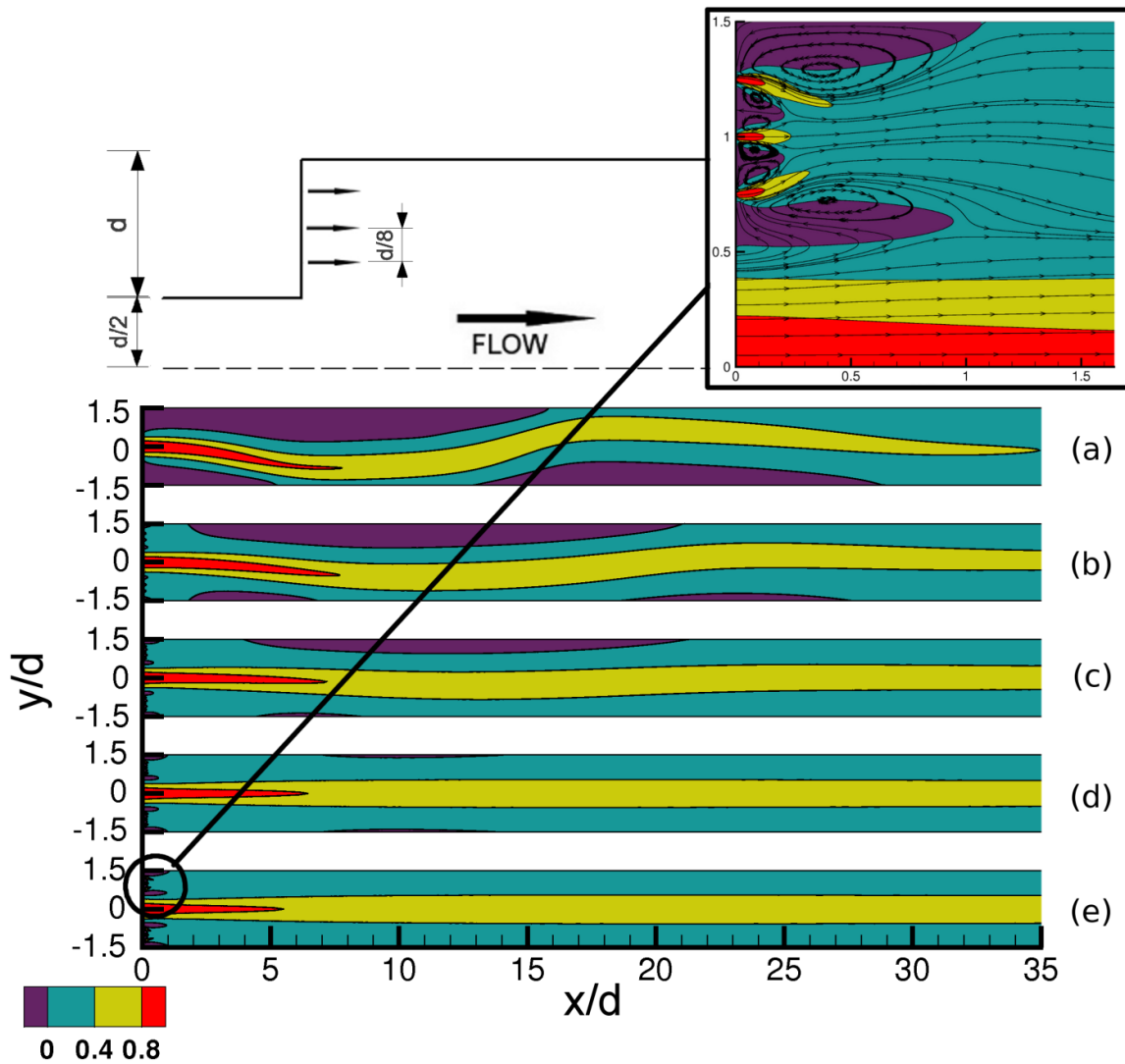


Figure 9. Axial velocity contours at $Re_c=380$ for various blowing configurations. Reference case $m_b/m_i = 0$ (a), case of $m_b/m_i = 0.18$ (b), case of $m_b/m_i = 0.27$ (c), case of $m_b/m_i = 0.315$ (d) and case of $m_b/m_i = 0.36$ (e).

Similar to the suction cases, the ordinates of U_{max} are shown for blowing cases in Figure 10. This figure shows that the flow stabilizes quickly as the blowing rate increases which is discerned from the decreasing peaks and is almost perfectly symmetric at $m_b/m_i=0.315$ since the ordinate is zero throughout the domain. It is understood that Figure 10 alone is not sufficient to judge whether the flow is free from the separation zones located near the upper and lower walls. For both cases (d) and (e), the ordinate is zero but we do still see these separation zones in the case (d) but not in the case (e).

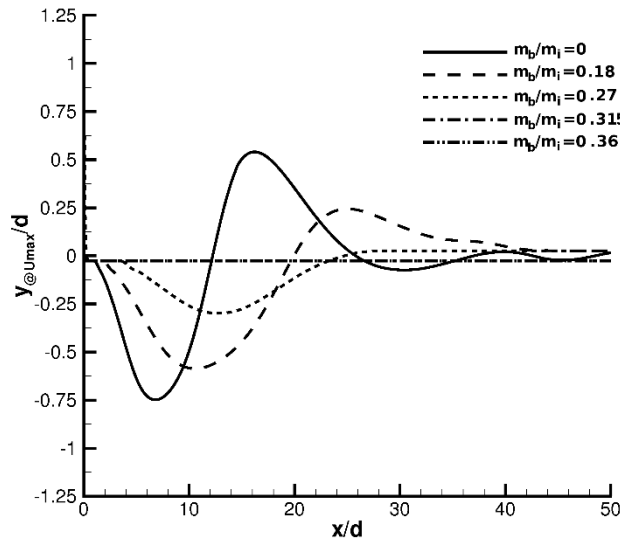


Figure 10. Variation of the location of maximum axial velocity $y@U_{max}/d$ for the blowing cases

4. CONCLUSION

The effort shown for the validation of the adopted code and the numerical method in this study resulted in the fact that velocity profiles for a 3:1 sudden expansion agree well with the experimental data [3]. Bifurcation characteristics are also predicted well with those of [13] and [26]. Following the courage gained from the validation with previous studies; the effects of some control parameters, including velocity profile modification, wall-shaping, blowing/suction and wall heating/cooling are examined in detail. The conclusions found in this study for the $Re_c=380$ can be summarized as follows:

- a) It is clearly seen that the instability increases at high Reynolds numbers or at the cases of thicker inlet boundary layers. The magnitude of asymmetry (MA) decreases to 0.197 (8 % change) for the case $\delta/d=0.2$ and to 0.173 (19 % change) for the case $\delta/d=0.02$ in comparison to $MA=0.214$ for the case $\delta/d=0.5$.
- b) Asymmetric shaping was not found to enhance the stability compared to the symmetric shaping. For the particular case discussed for the parabolic shaping of $\alpha_s=75^\circ$, symmetric shaping was observed to decrease the separation regions by 26 %, however this is managed only by 12 with asymmetric shaping.
- c) Suction was found to worsen the flow stability in sudden expansion, whereas blowing accomplished to stabilize the flow totally by eliminating the asymmetry in the flow at $m_b/m_i=0.36$.

For the future studies, the author has the plan on studying the effects of the frequency blowing rates on the stability of the sudden expansion flow problem.

REFERENCES

- [1] Macagno EO, Hung TK. Computational and experimental study of adaptive annular eddy. J. Fluid Mech. 1967; 28, 43-64.
- [2] Iribarne A, Frantisak F, Hummel RL, Smith JW. An experimental study of instabilities and other flow properties of a laminar pipe jet. A.I.Ch.E. J. 1972; 18, 689-698.

- [3] Durst F, Melling A, Whitelaw JH. Low Reynolds number flow over a plane symmetric sudden expansion. *J. Fluid Mech.* 1974; 64(1), 111-128.
- [4] Cherdron W, Durst F, Whitelaw JH. Asymmetric flows and instabilities in symmetric ducts with sudden expansion. *J. Fluid Mech.* 1978; 84, 13-31.
- [5] Ouwa Y, Watanabe M, Asawo H. Flow visualization of a two-dimensional water jet in a rectangular channel. *J. Appl. Phys.* 1981;20(1), 243-247.
- [6] Fearn RM, Mullin T, Cliffe KA. Nonlinear flow phenomena in a symmetric sudden expansion. *J. Fluid Mech.* 1990; 211, 595-608.
- [7] Cliffe KA, Greenfield AC. Some comments on laminar flow in symmetric two dimensional channels. Harwell Rep. AERE-TP 939 1982.
- [8] Sobey IJ, Drazin PG. Bifurcations of two-dimensional channel flows. *J. Fluid Mech.* 1986; 171, 263-287.
- [9] Fuchs L. Incompressible vortex flows: non-uniqueness and hysteresis. In *Proc. Zntl. Conf. on Numerical Methods in Fluid Dynamics.* 1988.
- [10] Durst F, Pereira JCF, Tropea C. The plane symmetric sudden expansion flow at low Reynolds numbers. *J. Fluid Mechanics* 1993; 248, 567-581.
- [11] Alleborn N, Nandakumar K, Raszillier H, Durst F. Further contributions on the two-dimensional flow in a sudden expansion. *J. Fluid Mech.* 1997; 330, 169-188.
- [12] Drikakis D. Bifurcation phenomena in incompressible sudden expansion flows. *Phys. Fluids.* 1997; 9, 76.
- [13] Battaglia F, Tavener SJ, Kulkarni AK, Merkle CL. Bifurcation of low Reynolds number flows in symmetric channels. *AIAA Journal.* 1997; 35(1), 99-105.
- [14] Yang YT, Kuo CL. Numerical study of a backward-facing step with uniform normal mass bleed. *Int. J. Heat and Mass Transfer.* 1997; 40 (7), 1677-1686.
- [15] Abu-Nada E, Al-Sarkhi A, Akash, B, Al-Hinti. Heat Transfer and Fluid Flow Characteristics of Separated Flows Encountered in a Backward-Facing Step Under the Effect of Suction and Blowing. *J. Heat Transfer-Transactions of the ASME.* 2007; 129(11), 1517-1528.
- [16] Uruba V, Jonas P, Mazur O. Control of a channel-flow behind a backward-facing step by suction/blowing. *Int. J. Heat Fluid Flow.* 2006; 28 (4), 665-672.
- [17] Makiola B, Ruck B. Experimental Investigation of a Singlesided Backward-Facing Step Flow With Inclined Step Geometries. *Engineering Turbulence Modeling and Experiments.* Elsevier, New York, 1990; 487-497.
- [18] Wahba EM. Iterative solvers and inflow boundary conditions for plane sudden expansion flows. *Applied Mathematical Modelling.* 2007; 31, 2553-2563.
- [19] Navabi M. Three-dimensional asymmetric flow through a planar diffuser: Effects of divergence angle, Reynolds number and aspect ratio. *Int. Com. in Heat and Mass Transfer.* 2010; 37, 17-20.

- [20] Blasius H, Grenzschieben in Flüssigkeiten mit kleiner Reibung. Z. Math. Phys. 1908.; 56., 1-37. Engl. transl. in NACA TM 1256.
- [21] Fluent 6.2 User Guide, Fluent Inc, Lebanon, USA; 2001.
- [22] Chorin AJ. Numerical Solution of the Navier-Stokes Equations. Mathematics of Computation 1968; 22(104), 745-762.
- [23] Leonard BP, Mokhtari S. ULTRA-SHARP Nonoscillatory Convection Schemes for High-Speed Steady Multidimensional Flow. 1990; NASA TM 1-2568 (ICOMP-90-12), NASA Lewis Research Center.
- [24] Vandoormaal JP, Raithby GD. Enhancements of the SIMPLE Method for Predicting Incompressible Fluid Flows. Numer. Heat Transfer. 1984; 7, 147-163.
- [25] Patankar SV. Numerical Heat Transfer and Fluid Flows. Hemisphere Publishing Corporation, Washington DC, USA, 1980.
- [26] De Zilwa SRN, Khezzar L, Whitelaw JH. Flows through plane sudden-expansion. Int. J. Num. Meth. Fluids. 2000; 32, 313-329.